Check for updates

Facile synthesis of highly tunable monodispersed calcium hydroxide composite particles by using a two-step ion exchange reaction†

Chih-Hui Yang,[abc] Ya-Chin Wang,[ad] Ta-Chen Wang,[d] Yi-Ching Chang,[a] Yun-Chul Lin,[a] Pei-Fan Chen,[a] Wei-Jie Huang,[a] Hsin-Yi Wen,[a] Yu-Mei Lin,[ad] Wen-Shuo Kuo,[e] Yi-Ting Wang[a] and Keng-Shiang Huang [iD] *[d]

"Calcium hydroxide [$Ca(OH)_2$]" is a medicament frequently used for antimicrobial purposes in endodontic procedures, or it is used as a toxic-waste adsorbent in industry. $Ca(OH)_2$ particles produced through conventional methods are size untunable and have a wide size distribution and polygonal shape. In this paper, a novel and facile approach involving template-mediated synthesis and two-step ion exchange is proposed for uniform size $Ca(OH)_2$ composite particles generation. "Sodium-alginate (Na-alginate)" was used as a precursor, and monodisperse Na-alginate emulsions were formed through needle droplet or droplet microfluidic technology. After the first ion exchange step with the Ca^{2+} ions, "calcium-alginate (Ca-alginate)" particles were obtained. The Ca-alginate particles were intermediate reaction products and were designed to be the templates for ensuring the spherical shape and size of products. The OH^- ions were used for the second ion exchange step to fabricate $Ca(OH)_2$ composite particles. The results revealed that the $Ca(OH)_2$ composite particles were size tunable, had a spherical shape, and were monodisperse (with a relative standard deviation of less than 8%). The 3-(4,5-dimethylthiazol-2-yl)-2,5-diphenyl tetrazolium bromide (MTT) assay revealed that the $Ca(OH)_2$ composite particles were potential biocompatible materials.

1. Introduction

"Calcium hydroxide [$Ca(OH)_2$]" is applied broadly in wall painting,[1] stone and wood conservation,[2] rapid and high-volume water treatment, thermochemical energy storage in solar power plants,[3] and to enhance the thermal stability of carbon nano-tubes.[4] In addition, $Ca(OH)_2$ is a valuable material for reducing "sulfur dioxide (SO_2)" of flue gas,[5] controlling SO_2 emission during the incineration process[6] and the dry-desulfurization process,[7] and as an advanced material for biomedical applications. Particularly in clinical settings, $Ca(OH)_2$ is applied in antifungal and antimicrobial dressings against *Candida albicans*[8] and *Enterococcus faecalis*[9] infections, respectively.[10,11] It is especially used in endodontic treatment as

a biomaterial for pulp capping agents, root canal sealers, and intracranial medication.[12–14] For example, as a pulp capping agent, hydroxyl group in $Ca(OH)_2$ supplied an alkaline which allowed repair, calcification and mineralizing action. The activity of $Ca(OH)_2$ correlated to lethal effect of hydroxyl ions on microorganisms, thus it had activity against bacterial, endotoxin, fungal and biofilms.[15–17] In addition, $Ca(OH)_2$ facilitates the proliferation and survival of human stem cells in endodontics and dental traumatology.[18,19] Thus, $Ca(OH)_2$ is a multipurpose material with applications in several industries or in clinical medicine.

Generally, the preparation of $Ca(OH)_2$ mainly involves the reaction of water with certain calcium compounds such as "quick lime (CaO)", "calcium hydride (CaH_2)" or calcium metal, as follows:[20]

$$CaO + H_2O \rightarrow Ca(OH)_2$$
$$CaH_2 + 2H_2O \rightarrow Ca(OH)_2 + 2H_2$$
$$Ca + 2H_2O \rightarrow Ca(OH)_2 + H_2$$
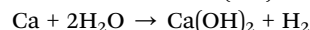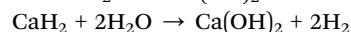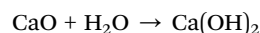
In addition, $Ca(OH)_2$ can be generated by hydrolyzing "calcium chloride ($CaCl_2$)" with "sodium hydroxide (NaOH)" at high temperatures, when diols (1,2-ethanediol or 1,2-propane-diol) are used as the reaction media.[21] Samanta *et al.* used "calcium nitrate dihydrate [$Ca(NO_3)_2 \cdot 2H_2O$]" as a calcium source, and then reacted it with NaOH to prepare $Ca(OH)_2$.[22] Chang showed that $CaCl_2$ was dissolved in heated deionized

[a]*Department of Biological Science and Technology, I-Shou University, Taiwan*

[b]*Pharmacy Department of E-Da Hospital, Taiwan*

[c]*Taiwan Instrument Research Institute, National Applied Research Laboratories, Taiwan*

[d]*The School of Chinese Medicine for Post-Baccalaureate, I-Shou University, No. 8, Yida Rd., Jiaosu Village Yanchao District, Kaohsiung City 82445, Taiwan. E-mail: huangks@isu.edu.tw; Tel: +886-988-399-979*

[e]*School of Chemistry and Materials Science, Nanjing University of Information Science and Technology, China*

water with less barium chloride and NaOH solution to obtain the primary filtrate. Then, pH was adjusted to 12.4–12.5 for the precipitation of $Ca(OH)_2$.[23] Furthermore, gelatin was used as a template to absorb solvated "calcium cations (Ca^{2+})" with coordination occurring between oxygen atoms and calcium cations to produce $Ca(OH)_2$ powder.[24,25] However, the aforementioned conventional methods have limitations such as particle size untunable, large particle size distribution, and polygonal particle shape. Generally, an additional centrifugation or filtration process is employed for overcoming the aforementioned limitations. However, these additional processes are inefficient.

Typically, shape, size and size distribution are a critical factor for applications.[26–28] Strom *et al.* demonstrated that from spherical $Ca(OH)_2$ particles, the slow release of calcium and hydroxide ions could be sustained for long periods to reduce the need for multiple visits by patients for apexification.[19] Developing a new approach to achieve monodispersed and flexible size-tunable spherical $Ca(OH)_2$ particles can make them suitable for the diverse applications. Thus, in this study, to produce $Ca(OH)_2$ particles, we proposed a new method involving template-mediated synthesis and a two-step ion exchange reaction.

2. Materials and methods

Materials

Na-alginate, sunflower seed oil, and $CaCl_2$ were purchased from Sigma Chemical Co. (MO, USA), Uni-President Enterprises Corp. (Taiwan), and J. T. Baker, respectively. NaOH, DMEM/F-12 medium, and $Ca(OH)_2$ reference were purchased from Mallinckrodt, GE Healthcare Life Science (Utah, USA), and AccuStandard, Inc. (CT, USA), respectively. Fibroblast cells (NIH/3T3) and human breast cancer cell lines (MCF-7) were purchased from Bioresource collection and research center (Food industry research and development institute, Taiwan).

Design and fabrication of a microfluidic chip

The microfluidic chip was fabricated by using AutoCAD 2007 (Autodesk, USA) and a CO_2 laser machine (LaserPro Venus, GCC, Taiwan) for constructing channel patterns on a "poly(-methyl methacrylate) (PMMA)" plate (length/width/depth: 270 mm/210 mm/1.5 mm), as described previously.[29–32] The microfluidic chip (length/width/depth: 86 mm/50 mm/6 mm) consisted of three PMMA chips, namely the cover chip (with three inlets for sample injection and twenty screw orifices for binding), the middle chip (with a cross-junction channel and twenty screw orifices), and the bottom chip (with an outlet and twenty screw orifices). The three chips were integrated using screws (0.5 mm pitch, 4 mm diameter), as illustrated by ESI Fig. S1.† The microfluidic chip could be disassembled for reuse and cleaning by loosening the screws.[29–32]

Synthesis of Ca-alginate thought needle droplets method

3 mL of 2% Na-alginate solution (0.2 g, dissolved in 10 mL of distilled water) was loaded in a syringe. Na-alginate emulsions were generated from the syringe tip by using a pump (speed, 12 mL h^{-1}) and the emulsions were then dropped into $CaCl_2$ solution (20 wt%). After 10 min, Ca-alginate particles were obtained. The particles were collected through centrifugation and were washed twice with 30 mL of distilled water.

Synthesis of Ca-alginate thought droplet microfluidics method

On a microfluidic chip, syringe pumps were employed for pumping 3 mL of 2% Na-alginate solution and 30 mL oil, which served as the water-phase and oil-phase fluids, respectively. After Na-alginate emulsions were generated, the emulsions were then transported and dropped into a 20% $CaCl_2$ solution. After 10 min, Ca-alginate spheres were collected through centrifugation and washed twice with 30 mL of distilled water.
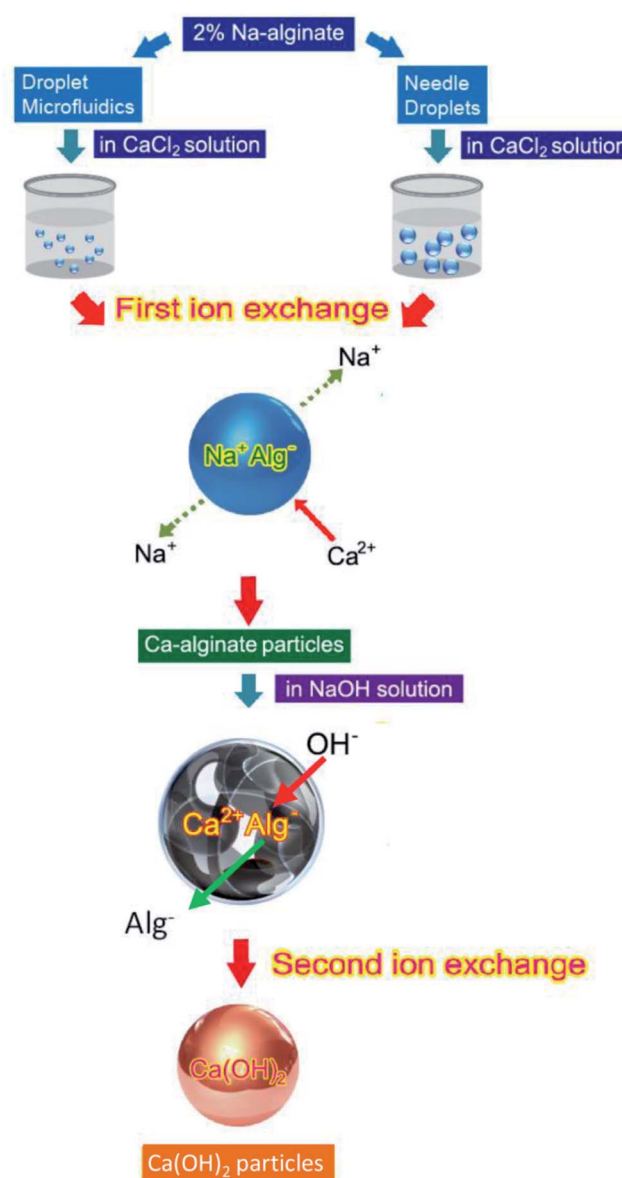

Fig. 1 Synthesis of $Ca(OH)_2$ composite particles by using two ion exchange steps.

Synthesis of spherical Ca(OH)$_2$ composite particles

Ca-alginate was employed both as the spherical shape template and as an intermediate of Ca(OH)$_2$. When Ca-alginate was dropped into 10 mL of 20% (w/v) NaOH solution for 20 min, Ca(OH)$_2$ composite particles could be observed. Distilled water (30 mL) was used to wash the Ca(OH)$_2$ composite particles three times. The Ca(OH)$_2$ composite particles were then immersed thoroughly in 10 mL of 65%, 75%, 85%, and then 95% alcohol, with each immersion lasting 20 min. Finally, dry Ca(OH)$_2$ composite particles were obtained.

Cytotoxicity test

Cell viability was evaluated using the "3-(4,5-dimethylthiazol-2-yl)-2,5-diphenyl tetrazolium bromide (MTT)" assay.[33,34] NIH/3T3 and MCF-7 cells (1×10^5 per well) were seeded into the 96-well culture dish plates containing 150 μL of the culture medium DMEM/F-12 (GE, USA) for 24 h. Before the MTT assay, the Ca(OH)$_2$ composite particles were ground to powder. Then, Ca(OH)$_2$ composite powder was mixed into DMEM/F-12 at concentrations ranging from 0 to 500 μg mL^{-1}. After 24 h, 150 μL of MTT solution (1 mg mL^{-1}) was added for a 4 h reaction with the cells at 37 °C. After removal of the medium and MTT, 150 μL of dimethyl sulfoxide was added to each well, and the assay plate was read at OD 595 nm on a microplate reader (Multiskan Ascent, Thermo Electron, Finland). The absorbance of the untreated cells in the control group was considered 100%.

Characterization

The average diameter of the particles is analyzed using photographs captured by a USB digital microscope (UPG621, Upmost, Taiwan) or a digital camera (DP70, Olympus, Japan). The average diameter of the spheres is expressed as "mean ± standard deviation (SD)". To minimize selection bias, 50 individual particles were sampled randomly. The morphology of the synthesized particles was analyzed using a "scanning electron microscope (SEM)" equipped with an "energy dispersive spectroscopy (EDS)" capability (Hitachi S-3400, Kyoto, Japan). "Fourier transform infrared (FTIR)" spectra were recorded using a Spectrum One FTIR spectrometer (PerkinElmer, Waltham, MA, USA) by employing KBr pellets in the range of 500–4000 cm^{-1}, with a resolution of 4 cm^{-1}. Moreover, X-ray diffraction (XRD, Bruker AXS Gmbh, Germany/D2 Phaser) patterns were obtained at room temperature by using Cu Kα radiation ($\lambda = 1.5406$ Å) with a range of $2\theta = 10°-65°$ and a scanning rate of 0.05 s^{-1}.

3. Results

Fig. 1 illustrates the innovate process for synthesizing Ca(OH)$_2$ composite particles. Na-alginate was used as an initial material, and Na-alginate emulsions were prepared using needle droplet or droplet microfluidic methods. When the Na-alginate emulsions were treated with CaCl$_2$ for the first ion exchange reaction, Ca-alginate particles were obtained. The second ion exchange step was used for producing Ca(OH)$_2$ composite particles. The Ca-alginate intermediate and NaOH were used to provide Ca^{2+} ions and OH$^-$ ions, respectively. To control the shape of Ca(OH)$_2$ composite particles (target products) with spherical, the intermediate Ca-alginate particles were designed to be spherical. Thus, the Ca-alginate particles were used as both an intermediate product and a spherical template. Using needle droplet or droplet microfluidic technology, identical spherical Ca-alginate particles could be manufactured facilely. Constructing a high-quality spherical Ca-alginate template is crucial

Table 1 Comparisons of flow rates and diameters of Ca-alginate and Ca(OH)$_2$ by droplet microfluidic technology[a]

Flow rate of continuous phase (mL min^{-1})	Flow rate of dispersed phase (mL h^{-1})	Ca-alginate particles			Ca(OH)$_2$ composite particles		
		Average size (μm)	S.D. (μm)	R.S.D. (%)	Average size (μm)	S.D. (μm)	R.S.D. (%)
0.7	0.2	404.9	9.1	2.2	549.9	24.5	4.5
	0.16	389.3	7.3	1.9	488.8	19.3	3.9
	0.12	384.6	8.7	2.3	455.2	6.4	1.4
	0.08	369.4	8.8	2.4	420.9	12.6	2.9
0.6	0.2	429.8	9.8	2.3	582.3	16.7	2.8
	0.16	404.6	11.5	2.8	570.7	20.6	3.6
	0.12	399.1	12.7	3.2	510.9	13.9	2.7
	0.08	388.7	17.7	4.5	477.3	15.6	3.3
0.5	0.2	463.2	7.3	1.6	605.5	18.3	3.1
	0.16	462.1	6.8	1.5	598.9	16.8	2.8
	0.12	454.9	8.3	1.8	561.9	12.7	2.3
	0.08	454.4	19.8	4.4	496.2	36.2	7.3
0.4	0.2	506.6	17.1	3.4	657.7	13.7	2.1
	0.16	505.9	11.3	2.2	653.6	11.7	1.8
	0.12	500.5	13.4	2.7	623.3	17.1	2.7
	0.08	471.6	24.8	5.3	532.1	17.2	3.2

[a] S.D.: standard deviation, R.S.D.: relative standard deviation.

for ensuring the formation of monodispersed and spherical $Ca(OH)_2$ composite particles.

For controlling the dimension and shape of Ca-alginate particles, two droplet manufacture methods were used. Needle droplet[35,36] and droplet microfluidic[29,37–39] methods were used for achieving the spherical $Ca(OH)_2$ composite particles in millimetre or micrometre scales, respectively. Relationships among various flow rates of continuous and dispersed phase, and various particle sizes of Ca-alginate and $Ca(OH)_2$ composite particles are presented in Table 1. The needle droplet technique is effective for manufacturing millimetre-scale droplets. The droplet microfluidic technique is expert in micrometer scale
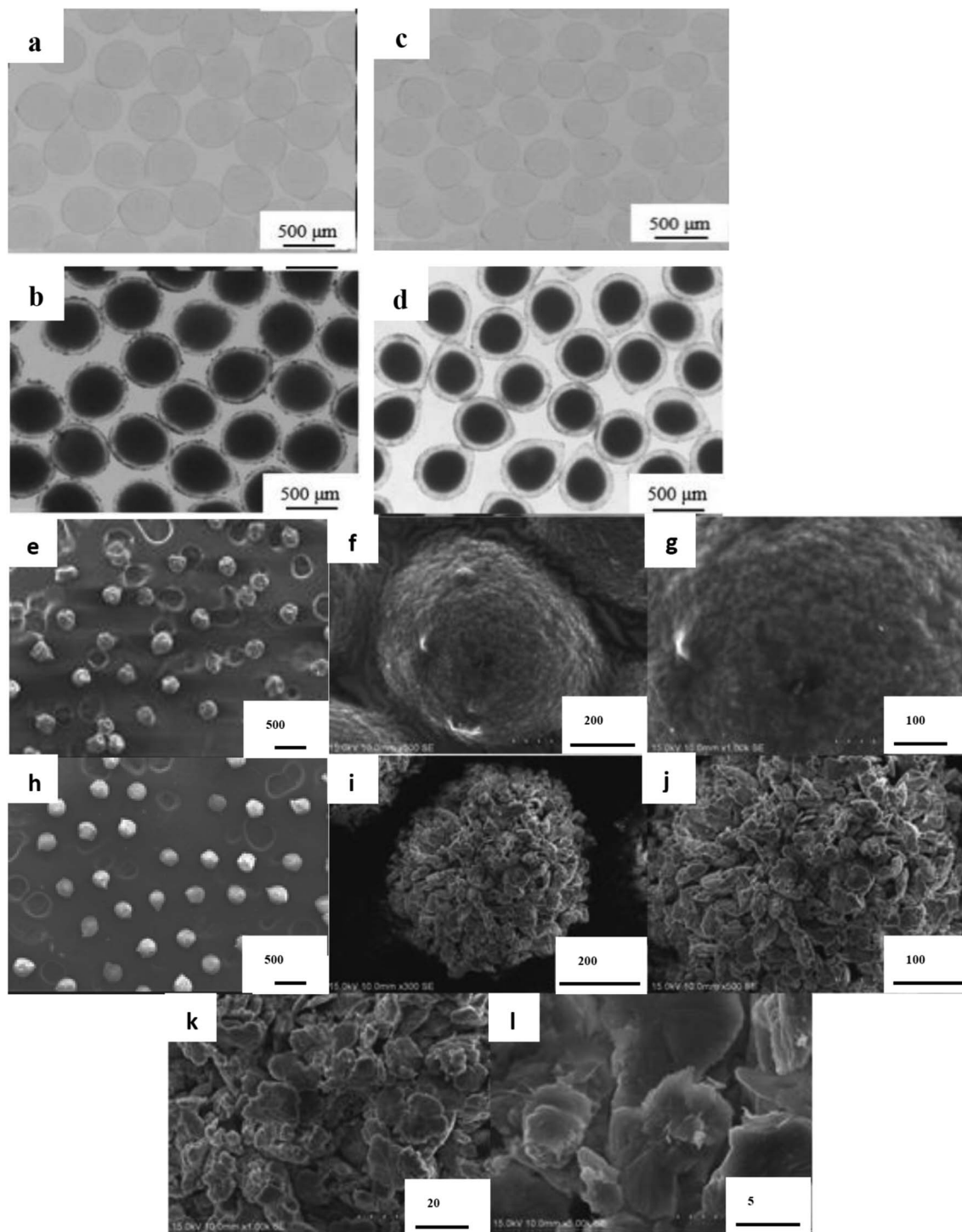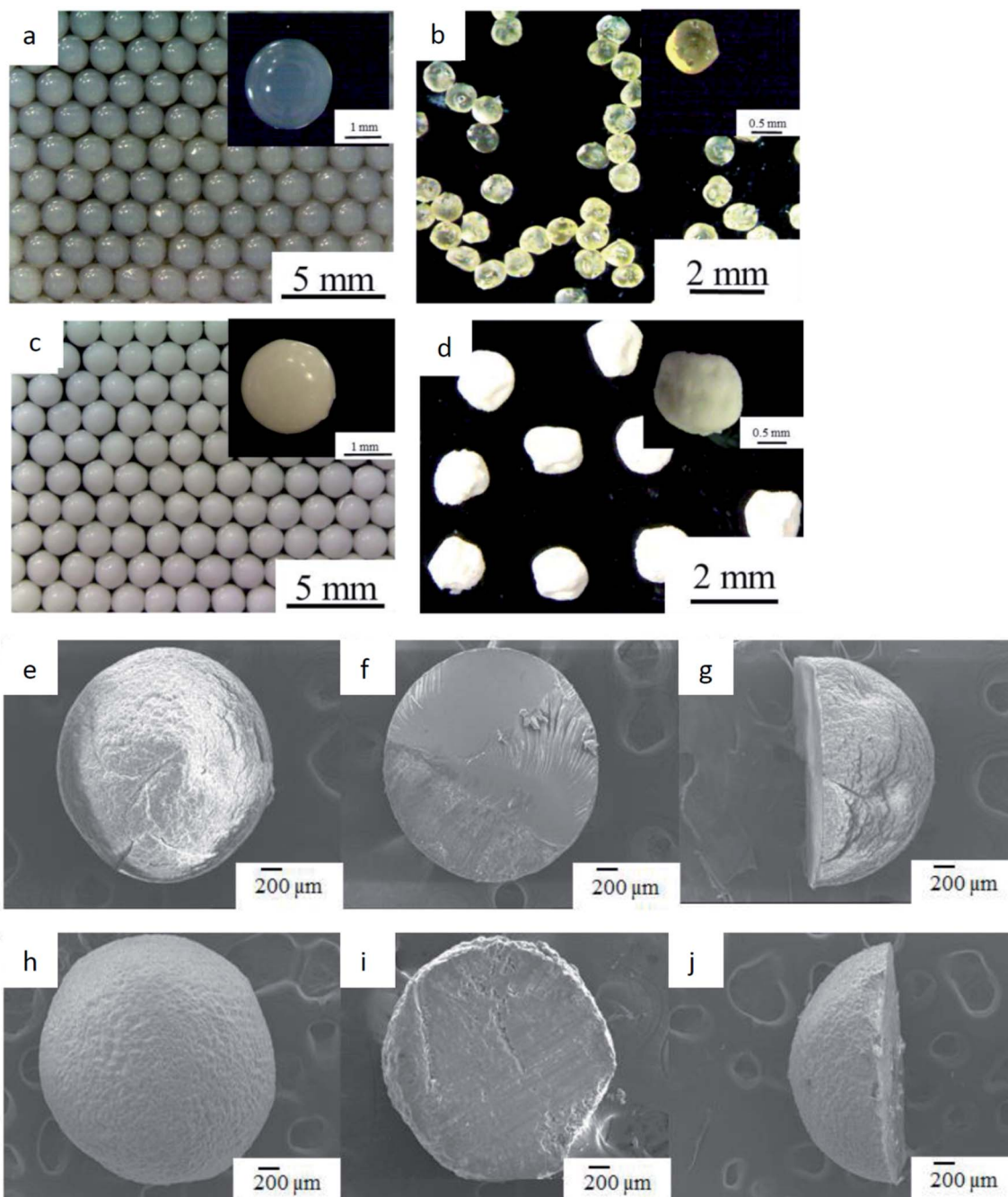

Fig. 2 Optical microscope and SEM images of Ca-alginate and $Ca(OH)_2$ composite particles, which prepared by using droplet microfluidic method. (a and c) Optical microscope images of wet Ca-alginate particles, (b and d) optical microscope images of wet $Ca(OH)_2$ composite particles; (e–g) SEM images of dry Ca-alginate particles, and (h–l) SEM images of dry $Ca(OH)_2$ composite particles.

droplets manufacture. In needle droplets, one can control droplets size by the size of the needle, flow rate, and viscosity of dispersed flow. For example, the 2.33 mm in diameter of Ca-alginate particles were obtained at a syringe flow of 1.2 mL h^{-1} and using a 24G ×1″ (0.55 × 25 mm) needle. The results show that controlling the diameter and shape of intermediate Ca-alginate enables controlling the diameter and shape of final product Ca(OH)$_2$ composite particles. The diameter of Ca(OH)$_2$ composite particles synthesized through needle droplet method was 2.01 ± 0.08 mm, with a "relative standard deviation (R.S.D.)" of 4.14%. In addition, the diameter of the Ca(OH)$_2$ composite particle synthesized through droplet microfluidic method ranged from 420.9 to 657.7 μm, with a R.S.D. of 1.4% to 7.3%. All the R.S.D. values were lower than 7.3%, indicating that

Fig. 3 Optical microscope and SEM images of Ca-alginate and Ca(OH)$_2$ particles, which prepared by using by needle droplet method. Optical microscope images of (a) wet Ca-alginate particles; (b) dry Ca-alginate particles; (c) wet Ca(OH)$_2$ composite particles; and (d) dry Ca(OH)$_2$ composite particles. SEM images of (e) full Ca-alginate particle; (f) top view of cross-sectional of Ca-alginate particle; (g) side view of cross-sectional of Ca-alginate particle; (h) full Ca(OH)$_2$ composite particle; (i) top view of cross-sectional of Ca(OH)$_2$ composite particle; (j) side view of cross-sectional of Ca(OH)$_2$ composite particle.
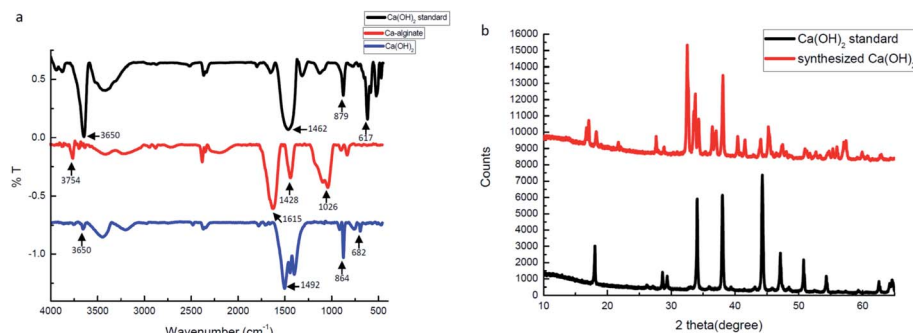
Fig. 4 (a) FTIR spectra of the $Ca(OH)_2$ standard, synthesized Ca-alginate particles and $Ca(OH)_2$ composite particles. (b) XRD patterns of the $Ca(OH)_2$ standard and synthesized $Ca(OH)_2$ composite particles.

the spherical particles meet the typical 10% R.S.D. criterion for monodispersed size distribution. The results revealed that all prepared spherical particles were uniform.

Optical and SEM images of the Ca-alginate and $Ca(OH)_2$ composite particles are provided in Fig. 2 and 3, respectively. The Ca-alginate and $Ca(OH)_2$ synthesized using droplet microfluidic method are depicted in Fig. 2a–d. Fig. 2a and c present Ca-alginate particles and reveal their transparent and spherical shape. Fig. 2b and d present $Ca(OH)_2$ composite particles, and reveal their spherical and non-transparency in the core and spherical and transparent in the shell. We conclude that the spherical type of the Ca-alginate particle template ensures the generation of spherical $Ca(OH)_2$ composite particles. According to magnified SEM images of the Ca-alginate depicted in Fig. 2e–g and of the $Ca(OH)_2$ depicted in Fig. 2h–l indicate different surface roundness. The $Ca(OH)_2$ composite particles depict compact slabs and flakiness on the particle surface.

Fig. 3a depicts the synthesized Ca-alginate particles with an average diameter of 2.33 ± 0.07 mm. The shrinkage rate between wet and dry Ca-alginate particles was approximately 41.2% (compared with Fig. 3a and b). Fig. 3c depicts the synthesized wet $Ca(OH)_2$ composite particles with an average diameter of 2.01 ± 0.08 mm. The shrinking rate between wet

and dry $Ca(OH)_2$ composite particles was approximately 17.6% (compared with Fig. 3c and d). The SEM images shown in Fig. 3e–j indicate that both Ca-alginate and $Ca(OH)_2$ composite particles were circular, spheroid, and solid. Internal ingredient of the prepared $Ca(OH)_2$ composite particle could be analyzed by using elemental mapping, please see ESI Fig. S2.†

FTIR spectra and XRD data were used to identify, analyze, and define the synthesized $Ca(OH)_2$ composite particles. Fig. 4a presents the FTIR spectra of the $Ca(OH)_2$ reference, the Ca-alginate and the $Ca(OH)_2$ composite particles. In $Ca(OH)_2$ reference (black curve), a sharp absorption peak at 3650 cm^{-1} was attributed to the hydroxyl group. The absorption peaks at 879 cm^{-1} and 617 cm^{-1} were assigned to different vibration of carbonate groups.[40] In Ca-alginate particles (red curve), the characteristic peaks at 1615 cm^{-1}, 1428 cm^{-1}, and 1026 cm^{-1} were observed.[41] In the synthesized $Ca(OH)_2$ composite particles (blue curve), the characteristic peaks at 1492 cm^{-1}, 864 cm^{-1} and 682 cm^{-1} were observed. The synthesised $Ca(OH)_2$ composite particles showed a characteristic peak at 880–680 cm^{-1}, which was attributed to Ca–O bending.[40]

Fig. 4b presents the XRD spectra, which confirmed that the synthesized composite particles were composed of $Ca(OH)_2$ crystalline phases because the positions and relative intensities
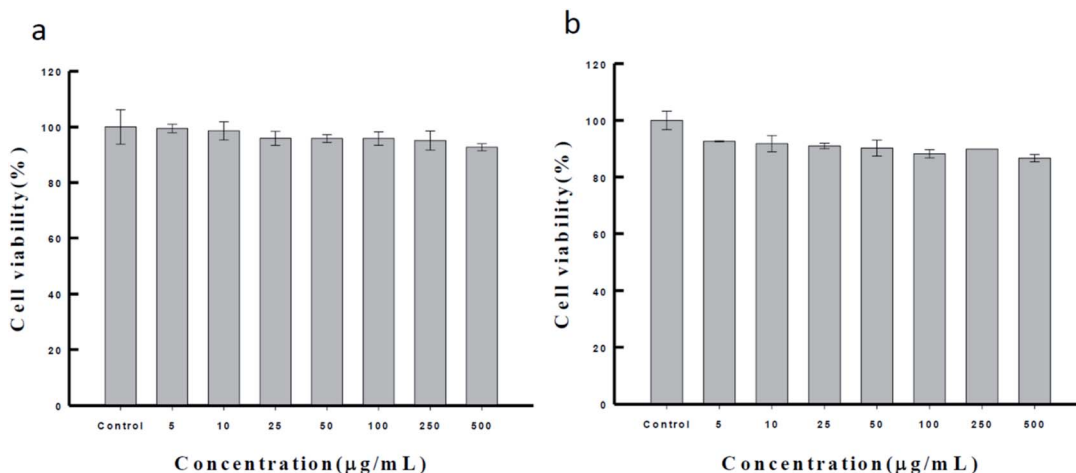

Fig. 5 The MTT assay of the synthesized $Ca(OH)_2$ composite particle in (a) NIH/3T3 cell and (b) MCF-7 cell, respectively.

of all diffraction peaks were consistent with the crystalline pattern of $Ca(OH)_2$.[42–44] The main peaks of the synthesized $Ca(OH)_2$ composite particles were consistent with those of the $Ca(OH)_2$ reference. The synthesized $Ca(OH)_2$ composite particles may not be pure enough, due to the presence of several extra peaks. Without purification, we presume that some Ca-alginate or Na-alginate may be present inside the $Ca(OH)_2$ composite particles. In ESI Fig. S3† weight losses of $Ca(OH)_2$ composite particles occurred from 30 to 275 °C, 275 to 580 °C and 580 to 750 °C, respectively. Weight loss at these three temperature ranges corresponded with the vaporisation of physically adsorbed water, the decomposition of $Ca(OH)_2$ to CaO, and the decomposition of $CaCO_3$ to CaO, respectively. We compared thermogravimetric data for synthesized $Ca(OH)_2$ with Ca-alginate, the purity of $Ca(OH)_2$ composite particles was approximately 80%.

Ca-alginate particles, the intermediator in our system, are biocompatible products used in the food industry.[45–47] For increasing the applicability of the $Ca(OH)_2$ composite particles as a biomaterial, we tested their biocompatibility through the MTT assay (as Fig. 5). MCF-7 and NIH/3T3 cells were cultured with the synthesized $Ca(OH)_2$ composite particles (0–500 μg mL^{-1}) for 24 h. The results show that the viability for both the NIH/3T3 and MCF-7 cells was approximately up to 90–99%. The biocompatible $Ca(OH)_2$ composite particles produced using the proposed method can be applied extensively in various treatment modalities in clinical medicine fields such as drug delivery systems.[15,48–52]

4. Conclusions

A new synthesis of $Ca(OH)_2$ composite particles thought an intermediary template and two ion exchange steps was proposed. In template-mediated synthesis, Ca-alginate particles were employed as a template for the controlling the shape and size of the final product (e.g. $Ca(OH)_2$ composite particles). The shape and size of the template could be controlled through needle droplet or droplet microfluidic methods, which produced size-tunable and spherical Ca-alginate particles. In the two-step ion exchange reaction, the Na-alginate reacted with Ca^{2+} ions, and Ca-alginate reacted with OH^- ions, respectively. After two ion exchange reactions, $Ca(OH)_2$ composite particles were obtained. All reactions were conducted at room temperature (~25 °C). Thus, our proposed facile method generated $Ca(OH)_2$ composite particles in the millimetre to micrometre scale. Future studies should investigate the use of droplet nanofluidics for nanoscale $Ca(OH)_2$ particle generation.

Author contribution statement

Yi-Ting Wang, Wen-Shuo Kuo, Hsin-Yi Wen, Yu-Mei Lin, Chih-Hui Yang, and Keng-Shiang Huang have written the main text and data analysis. Ta-Chen Wang, Yun-Chul Lin, Pei-Fan Chen, Yi-Ching Chang, Wei-Jie Huang and Ya-Chin Wang are experimental operations, prepared Figures and Table.

Conflicts of interest

The authors have declared no conflict of interest.

References

1 M. Ambrosi, L. Dei, R. Giorgi, C. Neto and P. Baglion, *Langmuir*, 2001, **17**, 4251–4255.

2 R. Giorgi, D. Chelazzi and P. Baglioni, *Langmuir*, 2005, **21**, 10743–10748.

3 D. Liu, L. Xin-Feng, L. Bo, Z. Si-quan and X. Yan, *Int. J. Energy Res.*, 2018, **42**, 4546–4561.

4 H. Kazemi, K. Zandi and H. Momenian, *J. Nanostruct.*, 2015, **5**, 25–32.

5 Y. Zhao, R. Hao, B. Yuan and J. Jiang, *J. Hazard. Mater.*, 2016, **301**, 74–83.

6 H. H. Tseng, M. Y. Wey and C. Y. Lu, *Environ. Technol.*, 2002, **23**, 109–119.

7 N. Matsushima, Y. Li, M. Nishioka, M. Sadakata, H. Qi and X. Xu, *Environ. Sci. Technol.*, 2004, **38**, 6867–6874.

8 R. J. Delgado, T. H. Gasparoto, C. R. Sipert, C. R. Pinheiro, I. G. de Moraes, R. B. Garcia, M. A. Duarte, C. M. Bramante, S. A. Torres, G. P. Garlet, A. P. Campanelli and N. Bernardineli, *Int. J. Oral Sci.*, 2013, **5**, 32–36.

9 M. Evans, J. K. Davies, G. Sundqvist and D. Figdor, *Int. Endod. J.*, 2002, **35**, 221–228.

10 R. Ordinola-Zapata, C. M. Bramante, P. G. Minotti, B. C. Cavenago, R. B. Garcia, N. Bernardineli, D. E. Jaramillo and M. A. Hungaro Duarte, *J. Endod.*, 2013, **39**, 115–118.

11 G. Sharma, H. M. A. Ahmed, P. S. Zilm and G. Rossi-Fedele, *Aust. Endod. J.*, 2018, **44**, 60–65.

12 A. Bystrom, R. Claesson and G. Sundqvist, *Endod. Dent. Traumatol.*, 1985, **1**, 170–175.

13 K. E. Safavi, W. E. Dowden, J. H. Introcaso and K. Langeland, *J. Endod.*, 1985, **11**, 454–456.

14 D. Kim and E. Kim, *Restor. Dent. Endod.*, 2014, **39**, 241–252.

15 Z. Mohammadi and P. M. H. Dummer, *Int. Endod. J.*, 2011, **44**, 697–730.

16 Z. Mohammadi, M. Soltani, S. Shalavi, M. Yazdizadeh and M. Jafarzadeh, *Compend Contin Educ Dent.*, 2014, **35**, 334–340.

17 Z. Mohammadi, H. Jafarzadeh, S. Shalavi, R. Sahebalam and J. I. Kinoshita, *J. Contemp. Dent. Pract.*, 2017, **18**, 246–249.

18 N. B. Ruparel, F. B. Teixeira, C. C. Ferraz and A. Diogenes, *J. Endod.*, 2012, **38**, 1372–1375.

19 T. A. Strom, A. Arora, B. Osborn, N. Karim, T. Komabayashi and X. Liu, *J. Dent. Res.*, 2012, **91**, 1055–1059.

20 M. Born, A. Chive and B. Delfort, *US Pat.*, US5756432, 1998.

21 B. Salvadori and L. Dei, *Langmuir*, 2001, **17**, 2371–2374.

22 A. Samanta, D. K. Chanda, P. S. Das, J. Ghosh, A. K. Mukhopadhyay and A. Dey, *J. Am. Ceram. Soc.*, 2015, **99**, 787–795.

23 W. L. Chang, China Pat., CN102390854, 2012.

24 M. Darroudi, M. Bagherpour, H. A. Hosseini and M. Ebrahimi, *Ceram. Int.*, 2016, **42**, 3816–3819.

25 S. U. Son, Y. Jang, K. Y. Yoon, E. Kang and T. Hyeon, *Nano Lett.*, 2004, **4**, 1147–1151.

26 M. Gaumet, R. Gurny and F. Delie, *Int. J. Pharm.*, 2007, **342**, 222–230.

27 A. Kikuchi and T. Okano, *Adv. Drug Deliv. Rev.*, 2002, **54**, 53–77.

28 A. Kikuchi, M. Kawabuchi, M. Sugihara, Y. Sakurai and T. Okano, *J. Controlled Release*, 1997, **47**, 21–29.

29 Y. S. Lin, K. S. Huang, C. H. Yang, C. Y. Wang, Y. S. Yang, H. C. Hsu, Y. J. Liao and C. W. Tsai, *PLoS One*, 2012, 7, e33184.

30 C. H. Yang, C. Y. Wang, A. M. Grumezescu, A. H. Wang, C. J. Hsiao, Z. Y. Chen and K. S. Huang, *Electrophoresis*, 2014, **35**, 2673–2680.

31 C. H. Yang, Y. S. Lin, K. S. Huang, Y. C. Huang, E. C. Wang, J. Y. Jhong and C. Y. Kuo, *Lab Chip*, 2009, **9**, 145–150.

32 C. H. Yang, L. S. Wang, S. Y. Chen, M. C. Huang, Y. H. Li, Y. C. Lin, P. F. Chen, J. F. Shaw and K. S. Huang, *Int. J. Pharm.*, 2016, **510**, 493–500.

33 A. Elbaz, J. Lu, B. Gao, F. Zheng, Z. Mu, Y. Zhao and Z. Gu, *Polymers*, 2017, **9**, 386–395.

34 K. S. Huang, C. H. Yang, Y. C. Wang, W. T. Wang and Y. Y. Lu, *Pharmaceutics*, 2019, **11**, 212–226.

35 C.-Y. Wang, C.-H. Yang, K.-S. Huang, C.-S. Yeh, A. H.-J. Wang and C.-H. Chen, *J. Mater. Chem. B*, 2013, **1**, 2205–2212.

36 B. Qian, M. Loureiro, D. A. Gagnon, A. Tripathi and K. S. Breuer, *Phys. Rev. Lett.*, 2009, **102**, 164502–164504.

37 Y. H. Kim, L. Zhang, T. Yu, M. Jin, D. Qin and Y. Xia, *Small*, 2013, **9**, 3462–3467.

38 K. S. Huang, K. Lu, C. S. Yeh, S. R. Chung, C. H. Lin, C. H. Yang and Y. S. Dong, *J. Controlled Release*, 2009, **137**, 15–19.

39 Y. S. Lin, C. H. Yang, C. T. Wu, A. M. Grumezescu, C. Y. Wang, W. C. Hsieh, S. Y. Chen and K. S. Huang, *Molecules*, 2013, **18**, 6521–6531.

40 M. Khachani, A. E. Hamidi, M. Halim and S. Arsalane, *J. Mater. Environ. Sci.*, 2014, **5**, 615–624.

41 P. S. Anbinder, L. Deladino, A. S. Navarro, J. I. Amalvy and M. N. Martino, *J. Encapsulation Adsorpt. Sci.*, 2011, **1**, 80–87.

42 K. M. Saoud, I. Ibala, D. E. Ladki, O. Ezzeldeen and S. Saeed, *Digital Heritage*, 2014, vol. 8740, pp. 342–352.

43 G. Taglieri, C. Mondelli, V. Danielel, E. Pusceddu and A. Trapananti, *Adv. Mater. Phys. Chem.*, 2013, **3**, 108–112.

44 S. Zhang, *RSC Adv.*, 2014, **4**, 15835–15840.

45 G. Dai, W. Wan, Y. Zhao, Z. Wang, W. Li, P. Shi and Y. Shen, *Biofabrication*, 2016, **8**, 025004.

46 N. Lin, A. Geze, D. Wouessidjewe, J. Huang and A. Dufresne, *ACS Appl. Mater. Interfaces*, 2016, **8**, 6880–6889.

47 N. Landazuri, R. D. Levit, G. Joseph, J. M. Ortega-Legaspi, C. A. Flores, D. Weiss, A. Sambanis, C. J. Weber, S. A. Safley and W. R. Taylor, *J. Tissue Eng. Regener. Med.*, 2016, **10**, 222–232.

48 L. Wang, S. Yang, J. Cao, S. Zhao and W. Wang, *Chem. Pharm. Bull.*, 2016, **64**, 21–26.

49 T. Schleeh, M. Madau and D. Roessner, *Carbohydr. Polym.*, 2016, **138**, 244–251.

50 F. Qu, M. Zhao, Y. Fang, K. Nishinari, G. O. Phillips, Z. Wu and C. Chen, *J. Sci. Food Agric.*, 2016, **96**, 4358–4366.

51 T. Komabayashi, R. N. D'Souza, P. C. Dechow, K. E. Safavi and L. S. W. Spångberg, *J. Endod.*, 2009, **35**, 284–287.

52 T. Komabayashi, C. Ahn, R. Spears and Q. Zhu, *J. Oral Sci.*, 2014, **56**, 195–199.